Multivariable Predictive Control of a Photobioreactor System

Mihaela Sbarciog*, George A. Ifrim†, Sergiu Caraman† and Alain Vande Wouwer*
*Automatic Control Laboratory, University of Mons,
Boulevard Dolez 31, 7000 Mons, Belgium
Email: MihaelaIuliana.Sbarciog@Umons.ac.be, Alain.VandeWouwer@Umons.ac.be
†Department of Automatic Control and Electrical Engineering "Dunarea de Jos" University of Galati,
Domneasca Street, no. 47, 800008, Galati, Romania
Email: George.Ifrim@Ugal.ro, Sergiu.Caraman@Ugal.ro

***Abstract*—This paper describes the implementation and validation of a model predictive controller (MPC) for a photobioreactor system. The microalgae concentration, the solution pH and the illumination index, which is related to the lit PBR volume, are simultaneously controlled at imposed setpoint values by manipulating the dilution rate, the flow of CO_2 supplied to the culture and the incident light. The complex, time consuming nonlinear optimization is replaced by iterative quadratic programming optimizations. With a reduced number of tuning parameters and no demand for dynamics decoupling, the proposed controller improves considerably the speed of the control loop compared to the results available in literature.**

I. Introduction

Cultures of microalgae have an interesting potential for the production of renewable energy. Their diversity accounts for a wide range of biofuels, i.e., biodiesel, biohydrogen, bioethanol, biogas. With lower requirements than other feedstocks, cultures of microalgae can reach higher yields in terms of fuel potential, and have lead to the concept of third-generation biofuels [1]. Microalgae can also be used to produce added-value compounds, such as long chain polyunsaturated fatty acids, neutral lipids, proteins, carbohydrates, pigments, vitamins etc. [2], [3]. Another major advantage of microalgae is their ability to use a variety of carbon sources for growth, and even more importantly, their potential to sustain photoautotrophic metabolism, using light as energy source to fix CO_2. In a context where CO_2 emissions from human activities are increasing, microalgae are solid candidates to achieve CO_2 mitigation. Thus, the importance of microalgae cultivation resides in their capacity to be redesigned as cell factories that require only solar light and inorganic substrates (i.e. CO_2, ammonia and phosphorus salts) to produce biofuels and added value compounds for food, feed, chemical and pharmaceutical sectors [4].

Nevertheless, reliable monitoring and control tools are required to sustainably develop microalgae industry towards achieving stable performance and process traceability [5]. To this end, the physico-chemical and biological phenomena involved in the process have to be translated into reliable mathematical models. In particular, the light-driven growth processes are described using a particular class of models that express the specific growth rate as a function of local irradiance. The radiative models, which express the light attenuation inside a culture of microalgae, are fundamental in photobioreactor studies [6]. The coupling between radiative models and growth kinetics is an active research topic and several dynamic models have been published [7], [8], [9], [10], [11].

Whereas the accurate modeling of microalgae cultivation has its elements of difficulty, the control of these processes is even more challenging. In addition to the typical nonlinear and complex characteristics of most biotechnological processes, specific limitations such as the heterogenous nature of the culture in terms of light distribution make the problem even more delicate to tackle. Recent results in the area of control of microalagae cultures include [12], [13], [14], [15], [16]. The biotechnological processes, and particularly the microalgae cultivation processes, are naturally multivariable and presents strong interactions between I/O channels requiring advanced control techniques to adapt to the dynamic changes in the structure of the system [17].

In this context, this study deals with the implementation and validation of a model predictive control (MPC) structure for a photobioreactor (PBR) system. MPC is particularly suited for controlling multivariable processes as it naturally considers the interconnections between the system inputs and outputs. The system outputs, i.e. biomass concentration, pH and the illumination index γ (the ratio between the lighted volume and the dark volume), are controlled by manipulating the dilution rate, the influent flow rate of carbon dioxide and the incident light intensity. In view of a future implementation on a real PBR system, a MPC algorithm is developed which approximates the complex time-consuming optimization by successive quadratic optimization. Compared to other control strategies implemented on the same model, the proposed solution improves considerably the response time.

The paper is organized as follows. Section II presents the mathematical model which describes the PBR system, while Section III introduces the MPC algorithm used to control the system. Simulation results are presented and discussed in Section IV and conclusions are drawn in Section V.

978-1-5090-4862-5/17/$31.00

II. Model Description

The mathematical model, which describes the growth of the microalgae in the photobioreactor consists of three parts [10]: the biological model, the radiative-transfer model and the thermodynamic model. The biological model describes the evolution of the system states X, c_{TIN}, c_{TIC}, c_{O_2}, $y_{out}^{CO_2}$ and $y_{out}^{O_2}$, which respectively represent the biomass concentration, total inorganic nitrogen concentration, total inorganic carbon concentration, dissolved oxygen concentration, molar fraction of carbon dioxide in the output gas and molar fraction of oxygen in the output gas:

$$\frac{dX}{dt} = r_x - DX \tag{1}$$

$$\frac{dc_{TIN}}{dt} = -\frac{Y_{N/X}}{M_x} r_x + D(c_{TIN,in} - c_{TIN}) \tag{2}$$

$$\frac{dc_{TIC}}{dt} = -\frac{1}{M_x} r_x + D(c_{TIC,in} - c_{TIC}) + (K_{La})_{O_2} \frac{D_{CO_2}}{D_{O_2}} \left(\frac{(y_{in}^{CO_2} + y_{out}^{CO_2})/2 \cdot P}{\gamma_{CO_2} H_{CO_2}} - c_{CO_2} \right) \tag{3}$$

$$\frac{dc_{O_2}}{dt} = \frac{Q_p}{M_x} - Dc_{O_2} + (K_{La})_{O_2} \left(\frac{(y_{in}^{O_2} + y_{out}^{O_2})/2 \cdot P}{H_{O_2}} - c_{O_2} \right) \tag{4}$$

$$\frac{dy_{out}^{CO_2}}{dt} = \frac{RT}{P \cdot V_g} \left(y_{in}^{CO_2} G_{in} - y_{out}^{CO_2} G_{out} - V_L (K_{La})_{O_2} \cdot \frac{D_{CO_2}}{D_{O_2}} \left(\frac{(y_{in}^{CO_2} + y_{out}^{CO_2})/2 \cdot P}{\gamma_{CO_2} H_{CO_2}} - c_{CO_2} \right) \right) \tag{5}$$

$$\frac{dy_{out}^{O_2}}{dt} = \frac{RT}{P \cdot V_g} \left(y_{in}^{O_2} G_{in} - y_{out}^{O_2} G_{out} - V_L (K_{La})_{O_2} \cdot \left(\frac{(y_{in}^{O_2} + y_{out}^{O_2})/2 \cdot P}{H_{O_2}} - c_{O_2} \right) \right) \tag{6}$$

In (1)- (6), D is the dilution rate, r_x is the photosynthetic growth rate, $c_{TIN,in}$ and $c_{TIC,in}$ respectively represent total inorganic nitrogen and total inorganic carbon concentrations in the influent, $y_{in}^{CO_2}$ and $y_{in}^{O_2}$ are respectively the molar fractions of carbon dioxide and oxygen at inlet; $Y_{N/X}$ is yield of total inorganic nitrogen (TIN) conversion, Q_p is the photosynthetic quotient, M_x is the C-mole mass; $(K_{La})_{O_2}$ represents the overall volumetric mass-transfer coefficient for oxygen, D_{CO_2} and D_{O_2} respectively represent the molecular diffusivity of carbon dioxide and of oxygen; P is the total pressure, R is the universal gas constant and T is the temperature; H_{CO_2} and H_{O_2} respectively represent the Henry's constant for CO_2 and for O_2; V_L and V_g are respectively the volume of liquid and of gas. G_{in} and G_{out} are the flows of gas at inlet and outlet, computed as

$$G_{in} = G_{in}^{CO_2} + G_{in}^{O_2} + G_{in}^{N_2} \tag{7}$$

$$G_{out} = G_{out}^{CO_2} + G_{out}^{O_2} + G_{out}^{N_2} \tag{8}$$

Based on (7), (8), the gas fractions in the inlet and outlet are respectively given by

$$y_{in}^{CO_2} = \frac{G_{in}^{CO_2}}{G_{in}} \quad y_{in}^{O_2} = \frac{G_{in}^{O_2}}{G_{in}} \quad y_{in}^{N_2} = \frac{G_{in}^{N_2}}{G_{in}} \tag{9}$$

$$y_{out}^{CO_2} = \frac{G_{out}^{CO_2}}{G_{out}} \quad y_{out}^{O_2} = \frac{G_{out}^{O_2}}{G_{out}} \quad y_{out}^{N_2} = \frac{G_{out}^{N_2}}{G_{out}} \tag{10}$$

Notice that nitrogen is neither produced nor consumed, thus its inlet flow rate equals its outlet flow rate. Hence

$$y_{in}^{N_2} \cdot G_{in} = y_{out}^{N_2} \cdot G_{out} \tag{11}$$

while (7), (9) and (8), (10) respectively imply that

$$y_{in}^{CO_2} + y_{in}^{O_2} + y_{in}^{N_2} = 1 \tag{12}$$

$$y_{out}^{CO_2} + y_{out}^{O_2} + y_{out}^{N_2} = 1 \tag{13}$$

The photosynthetic growth rate is highly dependent on the light availability inside the culture (G). Its attenuation along the PBR's depth (z) is expressed by a radiative-transfer model [7] coupled with a kinetic law, which allows to compute local photosynthetic responses based on the photon flux density q_0. The integration of the local photosynthetic responses provides an average photosynthetic response over the PBR's volume. Hence the photosynthetic growth rate is given by:

$$r_x = \frac{\mu_0}{L} \int_0^L \mu\left(G(z)\right) dz \cdot f(pH) \cdot X - \mu_s \cdot X \tag{14}$$

where

$$\mu\left(G(z)\right) = \frac{G(z)}{K_i + G(z)} \tag{15}$$

$$G(z) = q_0 \exp\left(-\frac{1+\alpha}{2\alpha} E_a X z \right) \tag{16}$$

$$f(pH) = \frac{(pH_{max} - pH)}{(pH - pH_{min})} \exp\left(1 - \frac{(pH_{max} - pH)}{(pH - pH_{min})} \right) \tag{17}$$

Using (15), (16) in (14), the photosynthetic growth rate can be rewritten as

$$r_x = \frac{\mu_0}{L} \cdot \frac{2\alpha}{(1+\alpha) E_a X} \ln\left(\frac{K_i + q_0}{K_i + q_0 \exp\left(-\frac{1+\alpha}{2\alpha} E_a X L\right)} \right) \cdot f(pH) X - \mu_s X \tag{18}$$

L, μ_0, μ_s, K_i are system parameters, $\alpha = \sqrt{E_a/(E_a + 2bE_s)}$ is the linear scattering modulus, E_a and E_s are respectively the mass absorption and mass scattering coefficients and b is the backward scattering fraction. The illumination index, defined as the ratio between the light zone and the total volume of the reactor [18] is given by:

$$\gamma = \frac{\ln\left(\frac{G_c}{q_0}\right)}{-\frac{1+\alpha}{2\alpha} \cdot E_a X \cdot L} \tag{19}$$

where G_c represents the irradiance at compensation point (where photosynthesis equals respiration).

The thermodynamic model refers to the $NH_3 - CO_2 - H_2O$ multisolute system, which quantitatively describes the molecular and ionic species, as well as the ionic activities. The interacting chemical species in the culture broth are: carbon dioxide

TABLE I
NUMERICAL VALUES OF THE PARAMETERS

Parameter	Value	Parameter	Value
E_a	172m^2/Kg	V_L	1.45e-3m^3
E_s	870m^2/Kg	V_g	1.74e-04m^3
b	0.0008	L	0.04m
μ_0	0.16h^{-1}	K_1	4.3766e-07
K_i	120μmol photon/m^2/s	K_2	4.6541e-11
μ_s	0.013h^{-1}	K_3	1.7619e-05
$Y_{N/X}$	0.181	K_4	3.0853
M_x	24.72e-3Kg/C-mol	K_W	1.0038e-14
Q_p	1.107	pH_{min}	4
$(K_La)_{O_2}$	0.9h^{-1}	pH_{max}	11
D_{CO_2}	1.96e-9m^2/s	γ_{CO_2}	1
D_{O_2}	2.5e-9m^2/s	$\gamma_{HCO_3^-}$	0.86
P	1.013e5Pa	$\gamma_{CO_3^{2-}}$	0.57
R	8.3143J/mol/K	γ_{OH^-}	0.88
T	298.15K	$\gamma_{NH_4^+}$	0.88
H_{CO_2}	2903.8Pa/m^3/mol	γ_{NH_3}	1
H_{O_2}	8.385e4Pa/m^3/mol	$\gamma_{NH_2COO^-}$	0.88
G_c	5μmol photon/m^2/s		

(c_{CO_2}), bicarbonate ions ($c_{HCO_3^-}$), carbonate ions($c_{CO_3^{2-}}$), ammonia(c_{NH_3}), ammonium ions ($c_{NH_4^+}$), carbamate ions ($c_{NH_2COO^-}$), hydroxyl ions (c_{OH^-}) and hydrogen ions (c_{H^+}). Hence, the mass balance of the species leads to

$$c_{TIN} = c_{NH_3} + c_{NH_4^+} + c_{NH_2COO^-} \tag{20}$$

$$c_{TIC} = c_{CO_2} + c_{HCO_3^-} + c_{CO_3^{2-}} + c_{NH_2COO^-} \tag{21}$$

Since the chemical reactions are much faster than the overall system dynamics, chemical equilibrium is assumed. The relationships between the species at chemical equilibrium are given in terms of species activities (products between activity coefficients and species concentrations):

$$K_1 = \frac{\gamma_{H^+} c_{H^+} \cdot \gamma_{HCO_3^-} c_{HCO_3^-}}{\gamma_{CO_2} c_{CO_2}}$$

$$K_2 = \frac{\gamma_{H^+} c_{H^+} \cdot \gamma_{CO_3^{2-}} c_{CO_3^{2-}}}{\gamma_{HCO_3^-} c_{HCO_3^-}}$$

$$K_3 = \frac{\gamma_{NH_4^+} c_{NH_4^+} \cdot \gamma_{OH^-} c_{OH^-}}{\gamma_{NH_3} c_{NH_3}}$$

$$K_4 = \frac{\gamma_{NH_3} c_{NH_3} \cdot \gamma_{HCO_3^-} c_{HCO_3^-}}{\gamma_{NH_2COO^-} c_{NH_2COO^-}}$$

$$K_W = \gamma_{H^+} c_{H^+} \cdot \gamma_{OH^-} c_{OH^-} \tag{22}$$

where K_i, $i \in 1, 2, 3, 4, W$ are the equilibrium constants. The charge balance equation and the calculation of the solution pH complete the thermodynamical model:

$$c_{NH_4^+} + c_{H^+} + c_{Na^+} = c_{HCO_3^-} + 2c_{CO_3^{2-}} + c_{NH_2COO^-} + c_{OH^-} + c_{Cl^-} \tag{23}$$

$$pH = -\log_{10}(\gamma_{H^+} c_{H^+}) \tag{24}$$

The numerical values of the system parameters are given in Table I.

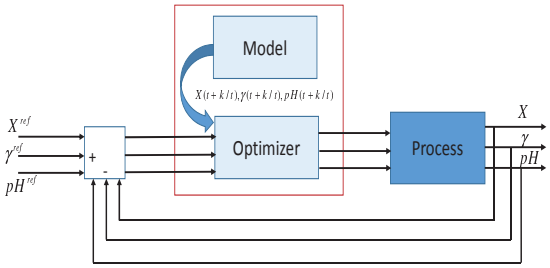

Fig. 1. The structure of the control loop

III. MULTIVARIABLE PREDICTIVE CONTROL

The successful use of MPC in advanced industrial applications lies in its ability to take into account constraints imposed on both process inputs (manipulated variables) and outputs (controlled variables), constraints which usually affect quality, economic efficiency and safety. Additionally, MPC techniques allow to address in a direct way the multivariable nature of the processes, the extension from single input single output to multiple inputs multiple outputs (MIMO) systems being straightforward. In this section we describe a MPC algorithm to control the biomass concentration (X), the pH of the solution (pH) and the illumination index (γ) of the PBR presented in Section II by manipulating the dilution rate (D), the inlet carbon dioxide gas flow rate ($G_{in}^{CO_2}$) and the photon flux density (q_0). Although it would be possible to assign for each controlled output a manipulated input and implement a non-cooperative predictive control algorithm, we present here the cooperative predictive control implementation, in which the set of inputs $(D, G_{in}^{CO_2}, q_0)$ is computed based on the total control error.

All predictive control algorithms are based on few common key elements: a system model to compute predictions of the controlled system outputs, the online optimization to find the optimal control variables and the feedback mechanism to compensate for disturbances affecting the system. The structure of the control loop employed here is shown in Fig. 1. The objective of a model predictive controller is to find the future process input sequence that optimizes a cost function over the prediction horizon N_p, taking the constraints on the process inputs and outputs into account. The simplest and most common cost index considers the summed squares of the predicted output deviations from the setpoint, although other terms such as penalties on the manipulated variables can also be included. The cost index considered here is

$$J = \sum_{k=1}^{N_p} \left(X^{ref}(t+k/t) - X(t+k/t)\right)^2 + \sum_{k=1}^{N_p} \left(pH^{ref}(t+k/t) - pH(t+k/t)\right)^2 + \sum_{k=1}^{N_p} \left(\gamma^{ref}(t+k/t) - \gamma(t+k/t)\right)^2 \tag{25}$$

where $X^{ref}(t+k/t)$, $pH^{ref}(t+k/t)$ and $\gamma^{ref}(t+k/t)$, $k=1\dots N_p$ denote the prediction of the respective setpoints made at time instant t, while $X(t+k/t)$, $pH(t+k/t)$ and $\gamma(t+k/t)$, $k=1\dots N_p$ denote the prediction of the respective process outputs made at time instant t. Since the process outputs are predicted using the model described in Section II, the minimization of the cost index J with respect to the process inputs D, $G_{in}^{CO_2}$, q_0 subjected to the constraints $D_{min}\le D\le D_{max}$, $G_{in,min}^{CO_2}\le G_{in}^{CO_2}\le G_{in,max}^{CO_2}$, $q_{0,min}\le q_0\le q_{0,max}$ results in a complex nonlinear optimization problem. The solution of this problem is difficult to get in due time in view of real-life implementation. Therefore we use here the algorithm described in [19], which replaces the complex, time consuming nonlinear optimization with iterative quadratic optimization problems, whose solutions converge to the nonlinear optimal solution.

Briefly, it is assumed that the future sequence of manipulated variables is the sum of a basic future control scenario and optimizing future control actions:

$$\begin{aligned}
&D(t+k/t)=D_{base}(t+k/t)+\delta D(t+k/t)\\
&G_{in}^{CO_2}(t+k/t)=G_{in,base}^{CO_2}(t+k/t)+\delta G_{in}^{CO_2}(t+k/t)\\
&q_0(t+k/t)=q_{0,base}(t+k/t)+\delta q_0(t+k/t)
\end{aligned}\tag{26}$$

$k=0\dots N_p-1$, which provide a first approximation of the output predictions as the cumulative result of the two effects:

$$\begin{aligned}
&X(t+k/t)=\bar{X}(t+k/t)+X_{opt}(t+k/t)\\
&pH(t+k/t)=p\bar{H}(t+k/t)+pH_{opt}(t+k/t)\\
&\gamma(t+k/t)=\bar{\gamma}(t+k/t)+\gamma_{opt}(t+k/t)
\end{aligned}\tag{27}$$

The response components $\bar{X}(t+k/t)$, $p\bar{H}(t+k/t)$ and $\bar{\gamma}(t+k/t)$, $k=1\dots N_p$ are computed by applying the known sequences $D_{base}(t+k/t)$, $G_{in,base}^{CO_2}(t+k/t)$, $q_{0,base}(t+k/t)$, $k=0\dots N_p-1$ to the model inputs, while the response components $X_{opt}(t+k/t)$, $pH_{opt}(t+k/t)$, $\gamma_{opt}(t+k/t)$ are given by the optimizing sequences $\delta D(t+k/t)$, $\delta G_{in}^{CO_2}(t+k/t)$, $\delta q_0(t+k/t)$. Assuming the optimizing components of the control actions inputs are small enough, it is possible to obtain an expression for $X_{opt}(t+k/t)$, $pH_{opt}(t+k/t)$, $\gamma_{opt}(t+k/t)$ by linearizing the model along the trajectories described by $D_{base}(t+k/t)$, $G_{in,base}^{CO_2}(t+k/t)$, $q_{0,base}(t+k/t)$. Hence, in matrix notations the prediction equations become

$$\begin{aligned}
&X=\bar{X}+G_{11}\cdot\delta D+G_{12}\cdot\delta G_{in}^{CO_2}+G_{13}\cdot\delta q_0\\
&pH=p\bar{H}+G_{21}\cdot\delta D+G_{22}\cdot\delta G_{in}^{CO_2}+G_{23}\cdot\delta q_0\\
&\gamma=\bar{\gamma}+G_{31}\cdot\delta D+G_{32}\cdot\delta G_{in}^{CO_2}+G_{33}\cdot\delta q_0
\end{aligned}\tag{28}$$

with

$$\begin{aligned}
&X=\left[\begin{array}{cccc} X(t+1/t) & \dots & X(t+N_p/t)\end{array}\right]'\\
&pH=\left[\begin{array}{cccc} pH(t+1/t) & \dots & pH(t+N_p/t)\end{array}\right]'\\
&\gamma=\left[\begin{array}{cccc} \gamma(t+1/t) & \dots & \gamma(t+N_p/t)\end{array}\right]'\\
&\bar{X}=\left[\begin{array}{cccc} \bar{X}(t+1/t) & \dots & \bar{X}(t+N_p/t)\end{array}\right]'\\
&p\bar{H}=\left[\begin{array}{cccc} p\bar{H}(t+1/t) & \dots & p\bar{H}(t+N_p/t)\end{array}\right]'\\
&\bar{\gamma}=\left[\begin{array}{cccc} \bar{\gamma}(t+1/t) & \dots & \bar{\gamma}(t+N_p/t)\end{array}\right]'\\
&\delta D=\left[\begin{array}{cccc} \delta D(t/t) & \dots & \delta D(t+N_p-1/t)\end{array}\right]'\\
&\delta G_{in}^{CO_2}=\left[\begin{array}{cccc} \delta G_{in}^{CO_2}(t/t) & \dots & \delta G_{in}^{CO_2}(t+N_p-1/t)\end{array}\right]'\\
&\delta q_0=\left[\begin{array}{cccc} \delta q_0(t/t) & \dots & \delta q_0(t+N_p-1/t)\end{array}\right]'
\end{aligned}\tag{29}$$

G_{ij}, $i,j\in\{1,2,3\}$ are the matrices of step response coefficients (i denotes the output, j denotes the input). By denoting

$$\begin{aligned}
&G_1=\left[\begin{array}{ccc} G_{11} & G_{12} & G_{13}\end{array}\right]\\
&G_2=\left[\begin{array}{ccc} G_{21} & G_{22} & G_{23}\end{array}\right]\\
&G_3=\left[\begin{array}{ccc} G_{31} & G_{32} & G_{33}\end{array}\right]\\
&U=\left[\begin{array}{ccc} \delta D & \delta G_{in}^{CO_2} & \delta q_0\end{array}\right]'
\end{aligned}\tag{30}$$

the cost index (25) can be rewritten in the standard form

$$J(U)=U'HU+2f'U+c\tag{31}$$

where

$$H=G_1'G1+G_2'G_2+G_3'G_3\tag{32}$$

$$\begin{aligned}
f&=-(G_1'(X^{ref}-\bar{X})+G_2'(pH^{ref}-p\bar{H})+G_3'(\gamma^{ref}-\bar{\gamma}))\\
c&=(X^{ref}-\bar{X})'(X^{ref}-\bar{X})+\\
&\quad(pH^{ref}-p\bar{H})'(pH^{ref}-p\bar{H})+(\gamma^{ref}-\bar{\gamma})'(\gamma^{ref}-\bar{\gamma})
\end{aligned}$$

which can be solved using quadratic programming techniques. Since (27) are only approximations, the control sequences $D(t+k/t)=D_{base}(t+k/t)+\delta D(t+k/t)$, $G_{in}^{CO_2}(t+k/t)=G_{in,base}^{CO_2}(t+k/t)+\delta G_{in}^{CO_2}(t+k/t)$ and $q_0(t+k/t)=q_{0,base}(t+k/t)+\delta q_0(t+k/t)$ are suboptimal. By redefining $D_{base}(t+k/t)\equiv D(t+k/t)$, $G_{in,base}^{CO_2}(t+k/t)\equiv G_{in}^{CO_2}(t+k/t)$, $q_{0,base}(t+k/t)\equiv q_0(t+k/t)$ and recomputing iteratively the control law components by repeating the procedure at the same sampling instant until

$$\begin{aligned}
&|\delta D(t+k/t)|\le\epsilon_D\\
&|\delta G_{in}^{CO_2}|\le\epsilon_{G_{in}^{CO_2}}\\
&|\delta q_0(t+k/t)|\le\epsilon_{q_0}
\end{aligned}\tag{33}$$

an accurate approximation of the optimal control can be obtained [20].

IV. Simulation results and discussion

The model described in Section II has been implemented in Matlab as a system of 16 differential-algebraic equations: 6 ordinary differential equations for the PBR states, 2 algebraic equations related to the gaseous system and 8 algebraic equations associated with the chemical species in the culture. The predictive controller, also implemented in Matlab, computes at every sampling instant $T_s=1$h new values for the process inputs, which are constrained as follows: $D\in[0,0.5]\text{h}^{-1}$, $G_{in}^{CO_2}\in[0,0.1]$mol/h, $q_0\in[0,1500]\mu$mol photon/m^2/s. A prediction horizon $N_p=5$ samples has been employed. The predictions of the setpoints over the prediction horizon have been set equal to the setpoint value at the present time instant, i.e. $X^{ref}(t+k/t)=X^{ref}(t)$, $pH^{ref}(t+k/t)=pH^{ref}(t)$, $\gamma^{ref}(t+k/t)=\gamma^{ref}(t)$. The bounds on the control increments

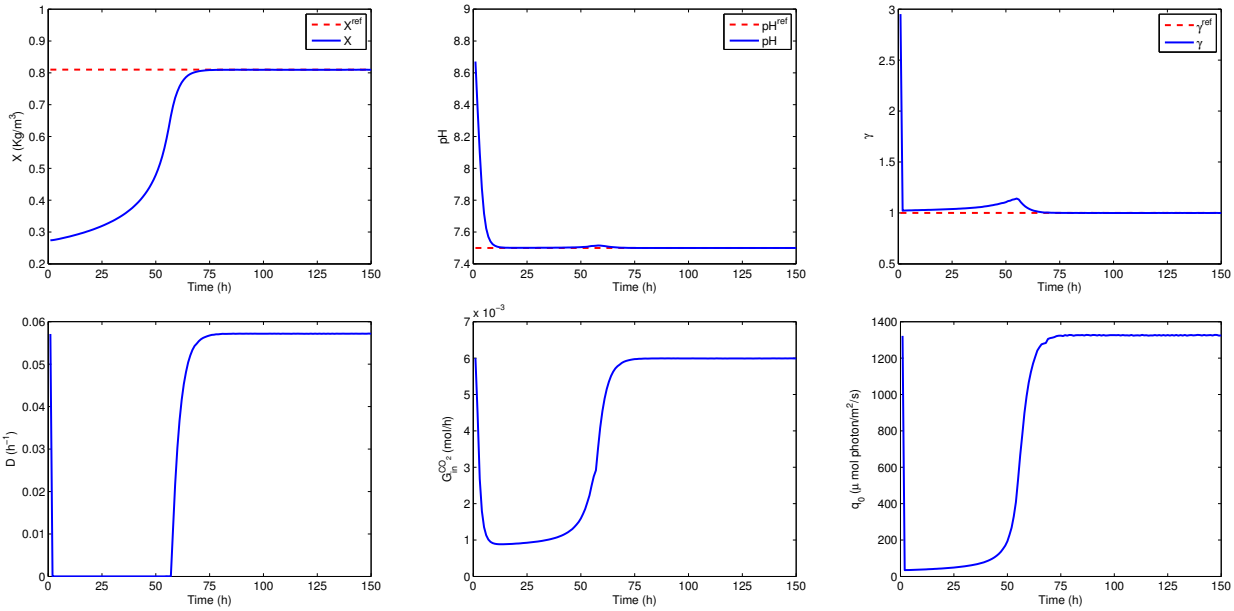

Fig. 2. Predictive control of the photobioreactor at optimal setpoint values

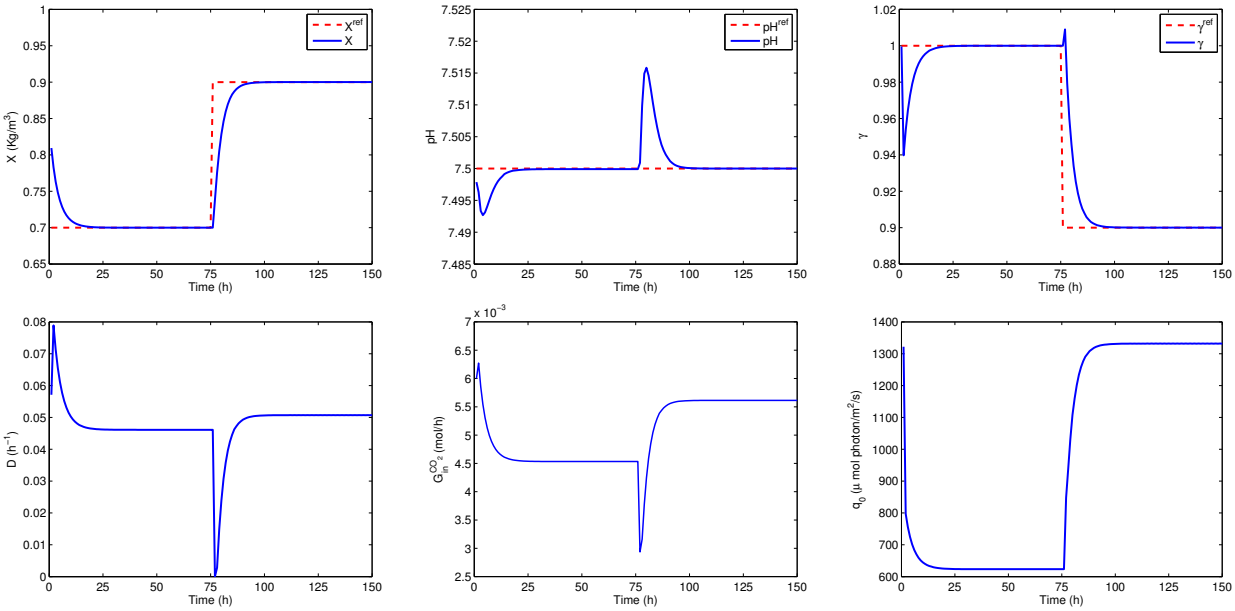

Fig. 3. Predictive control of the photobioreactor for several setpoint changes

have been defined as $\epsilon_D = 5 \times 10^{-4}$, $\epsilon_{G_{in}^{CO_2}} = 5 \times 10^{-5}$, $\epsilon_{q_0} = 4$. At each sampling instant, the optimization has been carried out until either conditions (33) were simultaneously fulfilled or a maximum of 30 QP-problems have been solved.

Figure 2 illustrates an experiment in which the setpoints for the controlled variables have been set to $X^{ref} = 0.81$Kg/m^3, $pH^{ref} = 7.5$ and $\gamma^{ref} = 1$, which represent an optimum situation as determined in [18]. Noticeably in Fig. 2 is that although the control of pH and γ can occur quite fast, a slight deterioration of the performance on these outputs is introduced by the controller to accelerate the control of the biomass concentration. This is a feature of cooperative predictive control approach, such as the one implemented here and it is not due to a badly tuned control loop. After 75h, all outputs have reached the imposed setpoints. Compared to the results published in [18] where X and γ reach their setpoints in 200h and 150h respectively, the proposed predictive controller improves considerably the speed of the loop. Figure 3 illustrates a second experiment which starts in the optimal conditions detailed before. In the first part of the experiment

a setpoint change is imposed on the biomass concentration while the pH and γ must be kept at the same setpoint values. In the second part of the experiment the setpoint values for biomass concentration and γ change at the same time instant. In all imposed scenarios, the multivariable MPC controller recomputes the optimal inputs and an effective control of the PBR system is obtained without the need of re-tuning the controller. The setpoint values for all controlled variables can be set independently, as long as they are reachable.

V. Conclusions

In this paper the multivariable predictive control of a complex photobioreactor system has been presented. The control loop has been implemented and evaluated in simulation. The obtained results indicate that the proposed control loop leads to better performances compared to the results available in literature. Aside the performance improvement that one may expect when using advanced control techniques, the emphasis in this paper was on using an algorithm which can provide an accurate approximation of the optimal control with sufficiently low computational effort. This requirement is of utmost importance in view of the envisaged real-life implementation of the control loop.

Acknowledgment

This work was carried out through the program "Partnerships in priority areas - PN II", implemented with the support of MECS - UEFISCDI, Project No. 269/2014 - BIOCON. M. Sbarciog acknowledges the support of MECS - UEFISCDI through the program "Mobility of young researches from diaspora" (PN-III-P1-1.1-MCT-2016-0044). This paper presents research results of the Belgian Network DYSCO (Dynamical Systems, Control, and Optimization), funded by the Interuniversity Attraction Poles Programme, initiated by the Belgian State, Science Policy Office. The scientific responsibility rests with the authors.

References

[1] J. Milano, H.C. Ong, H.H. Masjuki, W.T. Chong, M.K. Lam, P.K. Loh and V. Vellayan, "Microalgae biofuels as an alternative to fossil fuel for power generation," Renew. Sustainable Energy Rev., vol. 58, pp. 180 - 197, 2016.

[2] F. Alsenani and F. Ahmed, "Nutraceuticals from microalgae," in Nutraceuticals and Functional Foods in Human Health and Disease Prevention, D. Bagchi, H.G. Preuss and A. Swaroop, Eds. CRC Press, 2016, pp. 673-684.

[3] S.P. Cuellar-Bermudez, I. Aguilar-Hernandez, D.L. Cardenas-Chavez, N. Ornelas-Soto, M.A. Romero-Ogawa and R. Parra-Saldivar, "Extraction and purification of high-value metabolites from microalgae: essential lipids, astaxanthin and phycobiliproteins," Microb. Biotechnol., vol. 8(2), pp. 190-209, 2015.

[4] M.K. Lam, K.T. Lee and A.R. Mohamed, "Current status and challenges on microalgae-based carbon capture," Int. J. Greenhouse Gas Control, vol. 10, pp. 456-469, 2012.

[5] O. Bernard, "Hurdles and challenges for modelling and control of microalgae for CO2 mitigation and biofuel production," J. Process Contr., vol. 21(10), pp. 1378-1389, 2011.

[6] E. Lee, R.-L. Heng and L. Pilon, "Spectral optical properties of selected photosynthetic microalgae producing biofuels," J. Quant. Spectrosc. Radiat. Transfer, vol. 114, pp. 122-135, 2013.

[7] J.F. Cornet and C.G. Dussap, "A simple and reliable formula for assessment of maximum volumetric productivities in photobioreactors," Biotechnol. Progr., vol. 25(2), pp. 424-435, 2009.

[8] S. Fouchard, J. Pruvost, B. Degrenne, M. Titica and J. Legrand, "Kinetic modeling of light limitation and sulfur deprivation effects in the induction of hydrogen production with Chlamydomonas reinhardtii: part I. Model development and parameter identification," Biotechnol. Bioeng., vol. 102(1), pp. 232-245, 2009.

[9] J. Pruvost, J.F. Cornet, V. Goetz and J. Legrand, "Modeling Dynamic Functioning of Rectangular Photobioreactors in Solar Conditions," AIChE Journal, vol. 57(7), pp. 1947-1960, 2011.

[10] G.A. Ifrim, M. Titica, G. Cogne, L. Boillereaux, J. Legrand and S. Caraman, "Dynamic pH Model for Autotrophic Growth of Microalgae in Photobioreactor: A Tool for Monitoring and Control Purposes," AIChE J., vol. 60(2), pp. 585-599, 2014.

[11] A. Nikolaou, P. Hartmann, A. Sciandra, B. Chachuat and O. Bernard, "Dynamic coupling of photoacclimation and photoinhibition in a model of microalgae growth," J. Theor. Biol., vol. 390, pp. 61-72, 2016.

[12] S. Tebbani, F. Lopes, R. Filali, D. Dumur and D. Pareau, "Nonlinear predictive control for maximization of CO_2 bio-fixation by microalgae in a photobioreactor," Bioprocess Biosyst Eng., vol. 37(1), pp. 83-97, 2014.

[13] S. Tebbani, F. Lopes and G.B. Celis, "Nonlinear control of continuous cultures of Porphyridium purpureum in a photobioreactor," Chem. Eng. J., vol. 123, pp. 207-219, 2015.

[14] F. Mairet, R. Muñoz-Tamayo and O. Bernard, "Adaptive control of light attenuation for optimizing microalgae production," J. Process Contr., vol. 30, pp. 117-124, 2015.

[15] J.-S. Deschenes and A. Vande Wouwer, "Dynamic Optimization of Biomass Productivity in Continuous Cultures of Microalgae Isochrysis galbana through Modulation of the Light Intensity", *9th International Symposium on Advanced Control of Chemical Processes*, Whistler, Canada, 7-11 June, 2015.

[16] S.J. Yoo, D.H. Jeong, J.H. Kim and J.M. Lee, "Optimization of microalgal photobioreactor system using model predictive control with experimental validation," Bioprocess Biosyst. Eng., vol. 39(8), pp. 1235-1246, 2016.

[17] G.A. Ifrim, M. Titica, M. Barbu, L. Boillereaux, G. Cogne, S. Caraman and J. Legrand, "Multivariable feedback linearizing control of Chlamydomonas reinhardtii photoautotrophic growth process in a torus photobioreactor," Chem. Eng. J., vol. 218, pp. 191-203, 2013.

[18] G.A. Ifrim, M. Titica, M. Barbu, E. Ceanga and S. Caraman, "Optimization of a microalgae growth process in photobioreactors", 11th IFAC Symposium on Dynamics and Control of Process Systems, including Biosystems, Trondheim, Norway, 218-223, 2016.

[19] M. Sbarciog, I. Saraiva and A. Vande Wouwer, "Accelerating animal cell growth in perfusion mode by multivariable control: Simulation Studies", *Bioprocess and Biosystems Engineering* 36(5), 517-530, 2013.

[20] R.M.C. De Keyser, "Model based predictive control", Invited chapter in UNESCO Encyclopedia of Life Support Systems (EoLSS), article 6.43.16.1, vol 83. Eolss Publishers, Oxford, 2003.